J. Phys. B: At. Mol. Opt. Phys. **23** (1990) 1905-1913. Printed in the UK

Vibrational excitation of ethane by electron impact*

L Boesten†, H Tanaka‡, M Kubo§, H Sato‖, M Kimura¶#, M A Dillon¶ and D Spence¶

† Department of Physics, Sophia University, Chiyoda-ku, Tokyo, Japan 102
‡ Department of General Sciences, Sophia University, Chiyoda-ku, Tokyo, Japan 102
§ Matsushita Company, Osaka, Japan
‖ Ochanomizu University, Bunkyo-ku, Tokyo, Japan 112
¶ Argonne National Laboratory, Argonne, IL 60439, USA
# Department of Physics, Rice University, Houston, TX 77251, USA

Received 27 November 1989

Abstract. Differential cross sections for electron impact vibrational excitation of ethane (C_2H_6) have been determined for incident energies from 3 to 20 eV over a scattering angular range of 20° to 130°. In addition, vibrational excitation functions were determined for impact energies of 2 to 15 eV at scattering angles of 30°, 60°, 90° and 120°. These measurements confirm the broad shape resonance at 7.5 eV but provide no evidence for a (second) resonance near 2.3 eV. A decomposition of the vibrational energy-loss spectrum shows strong resonance enhancement of selected vibrational modes, which may be explained by decay of a temporary negative ion (TNI) of symmetry species e_u. A continuum multiple scattering calculation (CMS) reproduces these experimental results fairly well and indicates the simultaneous involvement of a TNI of species a_{2u}.

1. Introduction

Although vibrational excitation of saturated hydrocarbons by electrons of a few volts kinetic energy can be remarkably efficient, the physical mechanism leading to such large cross sections has not been studied in great detail.

Most previous investigations on the $e+C_2H_6$ system have been limited to Ramsauer techniques, swarm experiments or electron beam attenuation. For a brief survey of the literature up to 1985, see Curry *et al* (1985). The aim of all of these experiments was to provide accurate total cross sections rather than to separate elastic and inelastic effects in the electron-molecule interaction. Angular distributions of vibrationally inelastic scattering have been measured by Kubo *et al* (1981), Curry *et al* (1985) and Mapstone and Newell (1987). These measurements agree reasonably well with each other in the energy range from 7.5 to 20 eV for scattering angles from 30° to 130°. However, they relied for normalisation of their measurements on our outdated measurements of the elastic cross sections of ethane (Tanaka *et al* 1982).

To obtain improved quantitative measurements and to investigate resonant vibrational excitation near 7.5 eV in more detail, we have re-examined the differential cross sections (DCS) for vibrational excitation from 2 to 20 eV with an improved spectrometer. The vibrational excitation cross sections were normalised by comparison with elastic

* Work supported in part by the US Department of Energy, Assistant Secretary for Energy Research, Office of Health and Environmental Research and Office of Basic Energy Sciences, under Contract W-31-109-Eng-38, and by a Grant in Aid from the Ministry of Education, Science, and Culture, Japan.

0953-4075/90/111905+09$03.50

cross sections reported recently (Tanaka *et al* 1988, here after referred to as I). Neither the experiments nor the calculations give evidence to confirm a (second?) resonance near 2.3 eV reported previously (Christophorou 1980).

At present no theoretical treatment of molecular scattering can deal with a system as complicated as the e-ethane collision problem. In this study, we compare our experimental results with a recently developed continuum multiple scattering calculation modified to deal with target molecules of arbitrary complexity.

2. Experimental procedures

The spectrometer and experimental procedures were described in detail in I. The instrument employs a single-hemispherical monochromator and a similar analyser, computer-controlled lens voltages and differential pumping. In the present measurements the overall resolution was 32–40 meV, as indicated by the width of the elastic peak, and current intensity at the target was 2–20 nA, depending on impact energy. The incident electron energy was calibrated against the 19.37 eV resonance of He.

Figure 1 shows typical energy-loss spectra at a scattering angle of 90°. The first vibrational peak with a maximum at 0.18 eV energy loss encompasses the energies of vibrational modes (ν_2, ν_3, ν_6, ν_8, ν_9, ν_{11}, and ν_{12}) most of which are classified as 'deformations' (Herzberg 1945). The second peak with a maximum at 0.37 eV encompasses the energy range of modes ν_1, ν_5, ν_7 and ν_{10}, all of which can be roughly classified as stretching. In the following we refer to these two compound peaks as ν_b (bending, $\Delta E = 0.16$, different from the position of the maximum, see below) and ν_s (stretching, $\Delta E = 0.36$). The 'elastic' peak itself is slightly broadened by inclusion of ν_4 ($\Delta E = 0.034$ eV). Elastic scattering and energy-loss intensities were measured simultaneously and the ratio I_ν / I_0 of their integrated intensities (integration region ± 0.05 eV) was determined. This ratio is a good measure of the relative sizes of the corresponding cross sections. The I_0 value of the present measurements was then compared with I_0 of I in order to obtain the absolute differential cross sections for vibrational excitation.

For the measurements of vibrational excitation shown in figure 2, the analyser was set to transmit only electrons with an average loss of 0.16 eV (the centre of the left

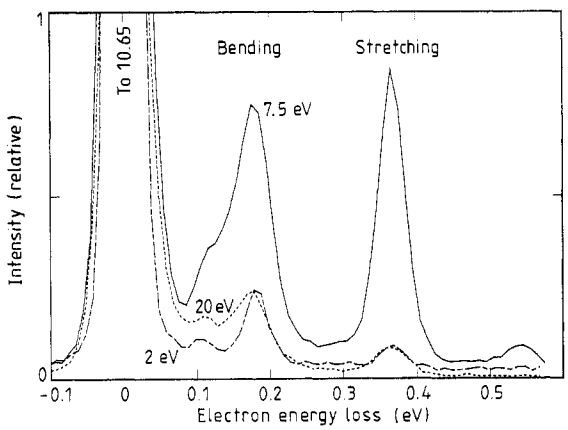

Figure 1. Electron energy-loss spectra of C_2H_6 at three different incident energies. There is a strong resonance enhancement of both vibrational compound modes ν_b and ν_s at 7.5 eV.

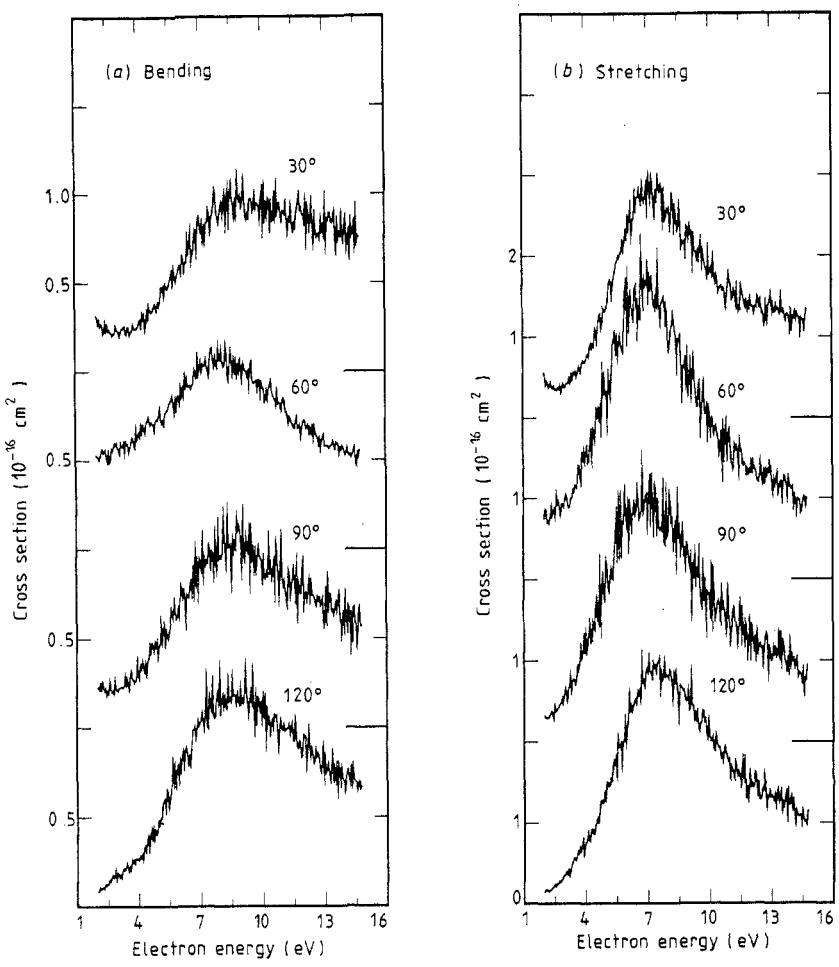

Figure 2. Excitation functions of the compound vibrational modes (a) ν_b, bending ($\Delta E = 0.16$ eV) and (b) ν_2, stretching ($\Delta E = 0.36$ eV).

compound peak), and to 0.36 eV for the right peak. Instrumental broadening then covers the full peaks, but note that the left vibrational peak rides on the tail of the elastic peak. The impact energy was swept from 2 to 14.75 eV at scattering angles of 30°, 60°, 90° and 120°. A novel technique described in Tanaka *et al* (1990) allows the direct determination of channel-by-channel normalised, absolute vibrational cross sections by alternating the C_2H_6 measurements at a given energy loss ΔE (0.16 or 0.36 eV) with He measurements at $\Delta E = 0$ eV. This technique assumes only that the transmission of the analyser lens system remains constant through the small shift in energy of size ΔE.

3. Experimental results

Figure 2 shows the excitation functions for the ν_b and ν_s overlapping modes at scattering angles of 30° to 120°. The profiles of these two excitation functions are similar and

remain unchanged over the experimentally observed angles, but there is a noticeable difference in peak location and shape between the two vibration modes. The bending modes peak at about 7.5 eV and the stretching modes at about 7.0 eV. We have observed a similar shift in peak location for CH_4. The peaks in the excitation functions correspond to the well known broad maximum in the total cross sections near 7.5 eV (cf I). This resonance also decays by dissociative electron attachment (cf Rutkowsky *et al* 1980), forming mainly H^- and CH_2^- with appearance potentials of about 8.3 and 9.2 eV (Von Trepka and Neuert 1963). The suggested dissociative channels imply the involvement of both C-C and C-H antibonding orbitals. Moreover, the large width (several eV) of these peaks indicates that the underlying resonance is rather short lived.

Figure 3 shows the angular dependence of the differential excitation cross sections of the ν_b and ν_s compound modes at incident energies from 3 to 20 eV. The same data are given in numerical form in table 1. The low-energy angular profiles show a structure slightly reminiscent of a d wave. At higher energies and lower angles there

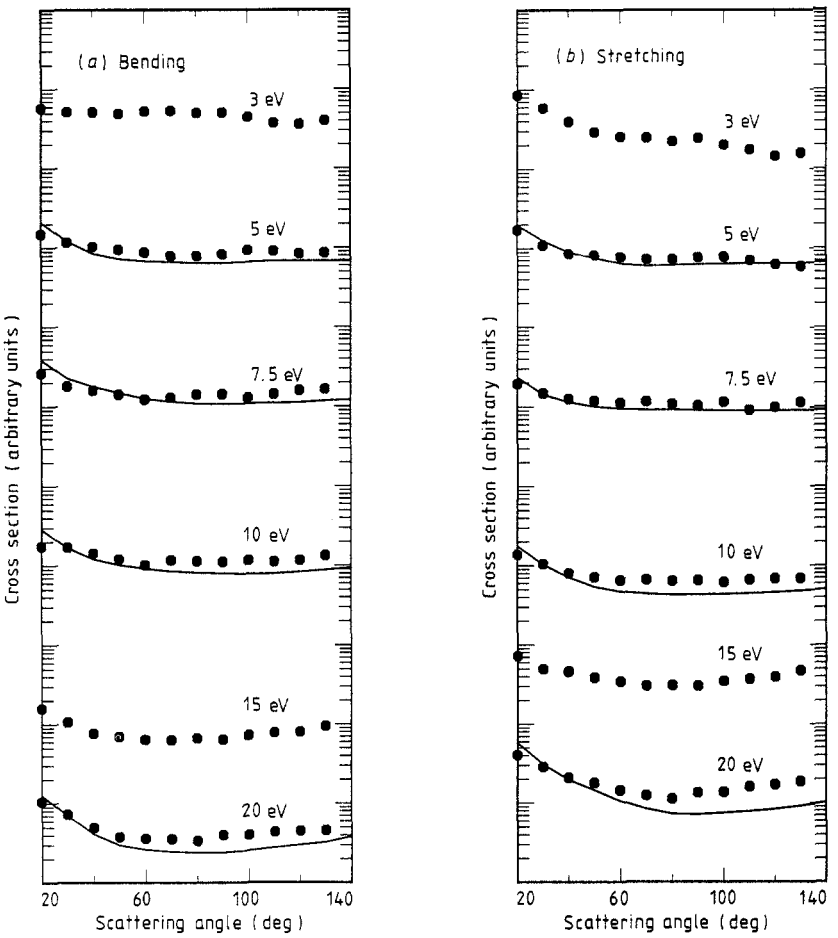

Figure 3. Angular distributions of the two compound vibrational modes (*a*) ν_b, bending ($\Delta E = 0.16$ eV) and (*b*) ν_s, stretching ($\Delta E = 0.36$ eV). The full curves are the results of our CMS calculation.

Table 1. Vibrational differential and integrated cross sections of C_2H_6 (in units of 10^{-16} cm^2 sr^{-1} and 10^{-16} cm^2)

	σ_b						σ_s					
θ/E	3	5	7.5	10	15	20	3	5	7.5	10	15	20
20	0.0576	0.149	0.262	0.175	0.158	0.105	0.0851	0.171	0.194	0.138	0.0725	0.0405
30	0.0518	0.117	0.181	0.170	0.107	0.0728	0.0587	0.110	0.148	0.105	0.0495	0.0286
40	0.0513	0.103	0.160	0.143	0.0763	0.0494	0.0396	0.0850	0.126	0.0798	0.0465	0.0209
50	0.0491	0.0948	0.141	0.126	0.0697	0.0379	0.0293	0.0819	0.119	0.0714	0.0386	0.0179
60	0.0524	0.0873	0.123	0.102	0.0641	0.0362	0.0256	0.0775	0.112	0.0652	0.0344	0.0145
70	0.0531	0.0782	0.129	0.117	0.0632	0.0357	0.0250	0.0732	0.119	0.0668	0.0305	0.0125
80	0.0500	0.0788	0.142	0.114	0.0669	0.0341	0.0225	0.0729	0.110	0.0643	0.0310	0.0113
90	0.0505	0.0826	0.143	0.112	0.0644	0.0402	0.0247	0.0772	0.105	0.0656	0.0305	0.0135
100	0.0444	0.0928	0.129	0.117	0.0728	0.0405	0.0203	0.0783	0.117	0.0616	0.0348	0.0137
110	0.0372	0.0905	0.143	0.112	0.0786	0.0440	0.0177	0.0711	0.093	0.0664	0.0371	0.0161
120	0.0360	0.0835	0.159	0.117	0.0802	0.0453	0.0147	0.0629	0.101	0.0687	0.0393	0.0171
130	0.0400	0.0860	0.166	0.134	0.0950	0.0460	0.0159	0.0594	0.116	0.0690	0.0472	0.0187
σ1	0.6038	1.1845	2.012	1.651	1.158	0.6482	0.3743	1.0222	1.483	0.9518	0.5517	0.2342

is an increase in cross sections from non-resonant (direct) excitation. At 15 eV and above, the tail rises in the fashion of a p wave.

The errors of the present DCS were estimated from the Poisson spread of the intensities entering the ratio I_ν/I_0 and the errors associated with the elastic DCS. The overall error is of the order of 20–35%.

In I we assumed that a short-lived shape resonance near 7.5 eV is the cause of the observed enhancement of the elastic DCS and attributed the resonance to an entrapment of the electron in one of the two lowest unoccupied antibonding orbitals, which would form a TNI of species A_{2u} or E_u (Caldwell and Gordon 1978). We concluded that the dominant partial wave would then be f ($l=3$), which also characterised the observed angular distribution in the region of the peak. The present measurements confirm the peak near 7.5 eV (see figure 2) and also allow us to draw more systematic conclusions about the partial wave composition of the scattered electron as well as the excited state.

The last row of table 1 contains the integral cross sections for the ν_b and ν_s compound modes. They were calculated from extrapolations obtained with a modified phaseshift (cf I) as well as by linear extrapolation along the last few measured values in a graph of log(DCS) against angle. The two fittings produced nearly identical results (maximum difference $<5\%$). The integrated cross sections of ν_b and ν_s agree rather well with those given by Hayashi (1989; based on swarm experiments), except at 20 eV. The overall error of the integrated cross sections is about 30%.

4. Symmetry considerations and decomposition of the energy-loss spectrum at resonance

Ethane belongs to the D_{3d} point group and has an A_{1g} ground state with an electron configuration $(\text{core})^4\text{-}2a_{1g}^2 2a_{2u}^2 1e_g^4$ symmetry. We let ψ_r, ψ_w, ψ_i, ψ_f and R, W, I, F represent the wavefunction and symmetry species of the trapped electron, the scattered electron wave, and the initial and final vibrational states. The previously mentioned two lowest unoccupied antibonding orbitals are $3a_{2u}$, $a\pi^*$ valence orbital mostly of the CH_3 group (6.84 eV, cf Snyder and Basch 1972, Robin 1974, Jorgensen and Salem 1973), and $2e_u$, $a\sigma^*$ orbital mostly of the C-C bond (10.01 eV). Following Wong and Schulz (1975), we suppose that the transition operator from ψ_i to ψ_f has the same symmetry as the charge density, $|\psi_r|^2$, of the additional electron. This assumption yields two possibilities: $a_{2u}\times a_{2u}=a_{1g}$ (case A), and $(e_u\times e_u)_s=a_{1g}$, e_g (case B; e_g is degenerate). If we now assume that species I is totally symmetric (a_{1g}), we obtain from direct product rules for the final state (A), $F=a_{1g}$, and for (B), $F=a_{1g}$, e_g. Finally, the symmetry species of the scattered electron wave can be calculated as $W\times F=R$ (Andrick and Read 1971), so that $W=a_{2u}$(A), or $W=e_u$; a_{1u}, a_{2u}, e_u(B). In either case A or case B, an expression of ψ_w in spherical harmonics will involve associated Legendre functions of odd degree only (Altmann 1957, Read 1968). Finally, the species of the final vibronic state $F=a_{1g}$ or e_g excludes many of the twelve vibrational modes of D_{3d} symmetry and hence constitutes strong selection. The allowed modes are listed in table 2.

At the previously established resonance energy of 7.5 eV, several vibrational modes become strongly resonance enhanced. This effect becomes most pronounced at 90° (see figure 1), but it also has been observed at other angles. In figures 4 and 5 we compare two decompositions of this energy-loss spectrum. The apparatus function was taken from the elastic peak. Rotational broadening and the inclusion of ν_4

Table 2. Representations of the symmetry species of the states involved in resonance.

	Representation			
State	Case A	Case B		
Excited state ψ_r	a_{2u}	e_u		
Final vibrational state ψ_f	a_{1g}	a_{1g}	or	e_g
Modes	ν_1, ν_2, ν_3	ν_1, ν_2, ν_3		$\nu_{10}, \nu_{11}, \nu_{12}$
Electron wave	a_{2u}	e_u	or	a_{1u}, a_{2u}, e_u
l	1, 3	1, 3		1, 3, 5

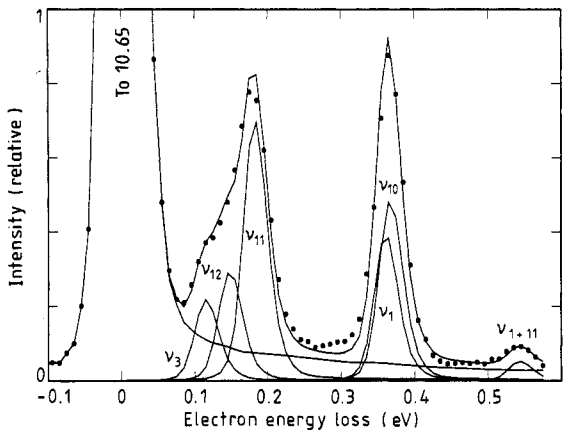

Figure 4. Decomposition of the energy-loss spectrum of figure 1 into vibrational modes ν_1, ν_2, ν_3, ν_{10}, ν_{11}, ν_{12} and ν_{1+11}. The weight of ν_2 is zero.

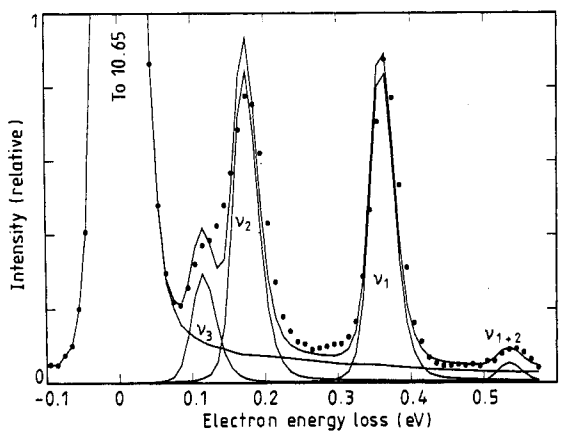

Figure 5. Same as figure 4 for vibrational modes ν_1, ν_2, ν_3 and ν_{1+2}.

(0.0358 eV) in the elastic peak were neglected. Problems arise only with the determination of the tail, which extends far into the region of the first vibrational excitation and whose size amounts to about 8% of the inelastic peak. The tail alters shape with a change in gas; thus the apparatus function had to be reconstructed from the loss spectrum itself. Small inaccuracies in the size and shape of the tail do not affect the following results.

In general, the theoretical determination of vibrational frequencies of complex molecules (cf Yamaguchi *et al* 1986, Hess *et al* 1984, both based on 6-31G* basis sets) and especially of ethane (Boatz and Gordon 1989, 3-21G basis set) is not precise enough for decomposition of experimental waveshapes. The frequency of all vibrational modes was therefore taken from a table in Martin and Montero (1984), who referred to the force field fittings to available experimental data from Duncan (1964). However, ν_3 had to be shifted from the listed 0.124 eV to 0.116 eV in order to perfectly match the shoulder at the left of the first peak. This was confirmed in a separate energy-loss spectrum taken at a different time with a different resolution (not shown).

The decomposition is sensitive enough to distinguish modes ν_{1+2} (0.5356 eV), ν_{1+11} (0.5442 eV) and ν_{10+11} (0.5508 eV) at the position of the small harmonic peak on the right of the figures. Figures 4 and 5 show clearly that three distinct features of the spectrum, namely the shoulder at the left of the first vibrational peak, the position of the second peak and the position of the harmonic at the far right, can only be accounted for by including vibrational modes ν_{10}, ν_{11} and ν_{12}, all of which belong to representation e_u (cf table 2). Note that these considerations do not exclude a simultaneous admixture of symmetry species a_{2u} (cf table 2).

5. Continuum multiple scattering calculation

The above conclusions were confirmed and extended by a continuum multiple scattering calculation (CMS; Kimura *et al* 1989, Sato *et al* 1988). In these calculations, a single parameter (the potential in the region between the atomic centres and the overall enclosing sphere) is adjusted once to obtain a best overall fit between theory and experiment for all energies and angles of elastic scattering. During vibrational calculations this parameter is held constant. While they are not rigorous *ab initio* calculations, the CMS calculations nevertheless are of great help in interpreting experimental data. A Hartree-Fock calculation showed that the two unoccupied orbitals $2e_u$ and $3a_{2u}$ are separated by less than 3 eV; thus, both states were included in the single-electron calculations by forming their coherent average (with equal weighting of their contributions). The results of the CMS calculations can be summarised as follows. The experimentally observed broad resonance peak around 7.5 eV is coincident with a large phaseshift excursion in the f-wave component of the a_{2u} and e_u scattering states. This peak is structureless because there are small differences (less than 1 eV) in the locations of the two resonances. Vibrational modes ν_3, ν_{11} and ν_{12} were included for the calculation of the compound mode ν_b and ν_1 and ν_{10} for compound mode ν_s (we know from the decomposition that ν_2 contributes very little). The lack of finer structure in the vibrational cross sections is mainly due to a nearly equal contribution of all partial waves, $l = 1, 3, 5$. As can be seen from figure 3, agreement between theory and experiment is reasonable (20-30%). Agreement could be improved by including further vibrational modes. However, the underlying physics seems to be correctly expressed by the present model.

6. Conclusion

The present work gives a broad range of quantitative measurements of the vibrational excitation of the ν_b and ν_s vibrational modes in ethane. The observed broad peak near 7.5 eV corresponds to a similar peak found in elastic scattering and indicates a short-lived shape resonance occurring in the σ^* orbital of the C-C valence bond and the π^* valence orbital of the CH_3 group. We expect similar but considerably modified results for disilane, further studies of which are underway.

References

Altmann S L 1957 *Proc. Camb. Phil. Soc.* **53** 343

Andrick D and Read F H 1971 *J. Phys. B: At. Mol. Phys.* **4** 389

Boatz J A and Gordon M S 1989 *J. Phys. Chem.* **93** 1819

Caldwell J W and Gordon M S 1978 *Chem. Phys. Lett.* **59** 403

Christophorou L G 1980 *Environm. Health Perspectives* **36** 3

Curry P J, Newell W R and Smith A C H 1985 *J. Phys. B: At. Mol. Phys.* **18** 2303

Duncan J L 1964 *Spectrochim. Acta* **20** 1197

Hayashi H 1989 Private communication

Hess A B, Schaad L J and Polavarapu P L 1984 *J. Am. Chem. Soc.* **106** 4348

Herzberg G 1945 *Infrared and Raman Spectra of Polyatomic Molecules* (New York: Van Nostrand)

Jorgensen W L and Salem L 1973 *The Organist Chemist's Book of Orbitals* (New York: Academic)

Kimura M, Sato H and Fujima K 1989 unpublished

Kubo M, Matsunaga D and Tanaka H 1981 *Proc. 12th Inf. Conf. on Physics of Electronic and Atomic Collisions (Gatlinburg)* (Amsterdam: North-Holland) Abstracts p 344

Mapstone I M and Newell W R 1987 *Proc. 15th Int. Conf. on Physics of Electronic and Atomic Collisions (Brighton)* (Amsterdam: North-Holland) Abstracts p 275

Martin J and Montero S 1984 *J. Chem. Phys.* **80** 4610

Read F H 1968 *J. Phys. B: At. Mol. Phys.* 1 893

Robin M B 1974 *Higher Excited States of Polyatomic Molecules* vol 1 (New York: Academic)

Rutkowsky J, Drost H and Spangenberg H-J 1980 *Ann. Phys.*, NY **37** 259

Sato H, Kimura M and Fujima K 1988 *Chem. Phys. Lett.* **145** 21

Snyder L C and Basch H 1972 *Molecular Wavefunctions and Properties* (New York: Wiley)

Tanaka H, Boesten L, Matsunaga D and Kudo T 1988 *J. Phys. B: At. Mol. Opt. Phys.* **21** 1255

Tanaka H, Boesten L, Sato H, Kimura M, Dillon M A and Spence D 1990 *J. Phys. B: At. Mol. Opt. Phys.* **23** 577

Tanaka H, Okada T, Boesten L, Suzuki T, Yamamoto T and Kubo M 1982 *J. Phys. B: At. Mol. Phys.* **15** 3305

Von Trepka L and Neuert H 1963 *Z. Naturf.* **18a** 1295

Wong S F and Schulz G J 1975 *Phys. Rev. Lett.* **35** 1429

Yamaguchi Y, Frisch M, Gaw J and Schaefer H F III 1986 *J. Chem. Phys.* **84** 2262